Supplementary Material: A Paradigm Shift in Data Assimilation: Reinforcement Learning for Chaotic Systems

Mohamad Abed El Rahman Hammoud[a], Naila Raboudi[a], Edriss S. Titi[b,c], Omar Knio[d], Ibrahim Hoteit[a]

[a]*Physical Sciences and Engineering Division, King Abdullah University of Science and Technology, Thuwal, 23955, Saudi Arabia*
[b]*Department of Applied Mathematics and Theoretical Physics, University of Cambridge, CB3 0WA, Cambridge UK*
[c]*Department of Mathematics, Texas A &M University, 77843, College Station, Texas, USA*
[d]*Computer, Electrical and Mathematical Sciences and Engineering, King Abdullah University of Science and Technology, Thuwal, 23955, Saudi Arabia*

This PDF file includes:

Table S1
Figs. S1 to S4

*Corresponding author Email: ibrahim.hoteit@kaust.edu.sa

	γ	max grad norm	v_f	$n_{a,train}$
$(N/A,\ 5,\ I_{d,3\times3})$	0.9	0.9	0.7	100
$(N/A,\ 50,\ I_{d,3\times3})$	0.1	0.8	0.7	100
$(N/A,\ 100,\ I_{d,3\times3})$	0.1	0.9	0.7	100
$(\mathcal{N}(0,1),\ 50,\ I_{d,3\times3})$	0.9	0.95	0.95	1000
$(\mathcal{N}(0,2),\ 50,\ I_{d,3\times3})$	0.05	0.8	0.7	1000
$(\mathcal{N}(0,3),\ 50,\ I_{d,3\times3})$	0.1	0.9	0.9	1000
$(\mathcal{N}(0,1),\ 5,\ I_{d,3\times3})$	0.25	0.8	0.7	100
$(\mathcal{N}(0,1),\ 50,\ I_{d,3\times3})$	0.9	0.95	0.95	1000
$(\mathcal{N}(0,1),\ 100,\ I_{d,3\times3})$	0.05	0.95	0.9	1000
$(\mathcal{N}(0,1),\ 50,\ I_{d,3\times3})$	0.9	0.95	0.95	1000
$(\mathcal{L}(0,1),\ 50,\ I_{d,3\times3})$	0.8	0.85	0.95	100
$(\mathcal{U}(0,1),\ 50,\ I_{d,3\times3})$	0.1	0.9	0.8	100
$(\mathcal{N}(0,1),\ 50,\ diag(1,0,0))$	0.25	0.8	0.8	500
$(\mathcal{N}(0,1),\ 50,\ diag(1,1,0))$	0.3	0.9	0.7	500
$(\mathcal{N}(0,1),\ 50,\ diag(1,0,1))$	0.25	0.8	0.95	1000

Table 1: Table describing the hyperparameters used to train the RL agent using the proximal policy optimization algorithm. The table outlines the hyperparameters for all 15 experiments considered in the study. All agents were trained using the ADAM optimization algorithm with a learning rate of 10^{-3}. Moreover, all actor and critic networks are comprised of densely connected multilayer perceptrons with two hidden layers with 128 neurons each.

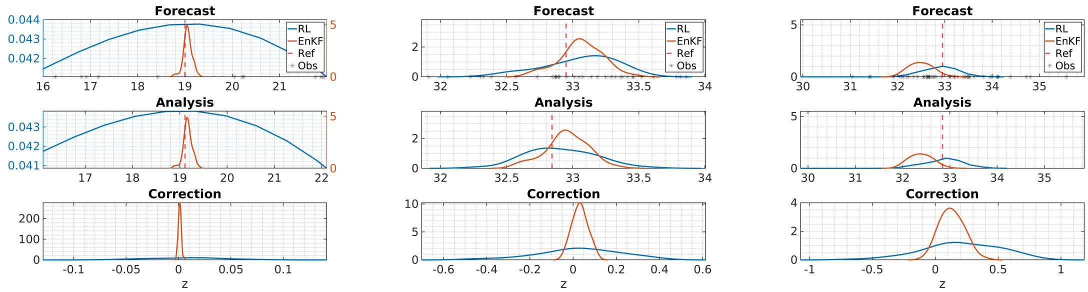

(a) $\left(\mathcal{N}(0,1),\ 5,\ I_{d,3\times3}\right)$ (b) $\left(\mathcal{N}(0,1),\ 50,\ I_{d,3\times3}\right)$ (c) $\left(\mathcal{N}(0,1),\ 100,\ I_{d,3\times3}\right)$

Figure 1: PDFs of the z-variable before (top) and after (middle) the correction step at time $t = 45$ alongside the PDF of the correction (bottom) for the EnKF and RL solutions. The plots are presented for the experiment analyzing the sensitivity of the data assimilation algorithms to assimilation frequency. As can be seen from the plots, the RL distributions for the z-variable and the correction are wider than that of the EnKF. Nevertheless, the RL distribution covers more of the noisy observations than the EnKF does. Furthermore, the mode of the RL ensemble is closer to the reference solution in comparison to the EnKF.

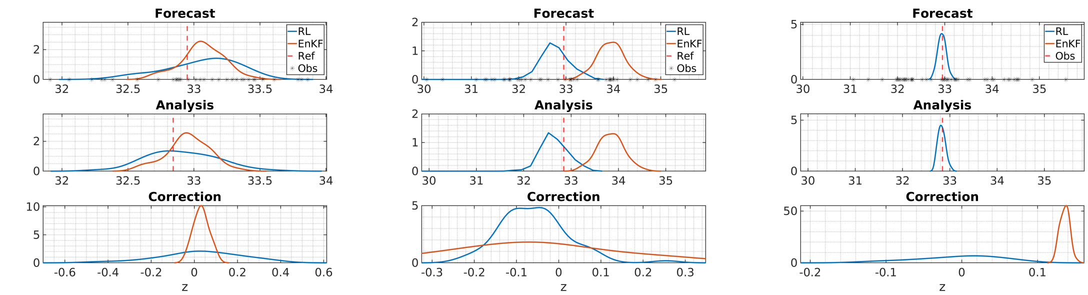

(a) $\left(\mathcal{N}(0,1),\ 50,\ I_{d,3\times3}\right)$ (b) $\left(\mathcal{L}(0,1),\ 50,\ I_{d,3\times3}\right)$ (c) $\left(\mathcal{U}(0,1),\ 50,\ I_{d,3\times3}\right)$

Figure 2: PDFs of the z-variable before (top) and after (middle) the correction step at time $t = 45$ alongside the PDF of the correction (bottom) for the EnKF and RL solutions. The plots are presented for the experiment analyzing the sensitivity of the data assimilation algorithms to the distribution of the observational noise. The plots indicate that while both the EnKF and RL distributions admit a high probability near the reference solution for the case of Gaussian noise, the RL solution is much closer to the reference solution than the EnKF solution in the case of lognormal and uniform noise. Furthermore, in the case of nongaussian noise, the EnKF correction term appears to be much more aggressive than that of RL and generally appears not to have a particular structure.

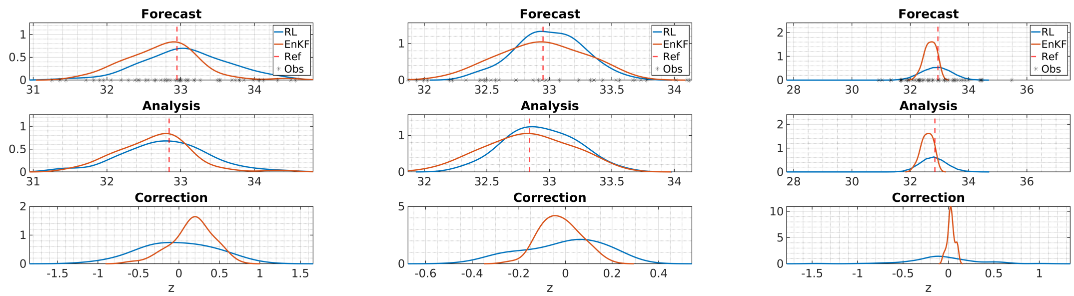

(a) $(\mathcal{N}(0,1),\ 50,\ diag(1,0,0))$ (b) $(\mathcal{N}(0,1),\ 50,\ diag(1,1,0))$ (c) $(\mathcal{N}(0,1),\ 50,\ diag(1,0,1))$

Figure 3: PDFs of the z-variable before (top) and after (middle) the correction step at time $t = 45$ alongside the PDF of the correction (bottom) for the EnKF and RL solutions. The plots are presented for the experiment analyzing the sensitivity of the data assimilation algorithms to partial observability. For the case of $\mathcal{H} = (1, 0, 0)$ and $(1, 1, 0)$, the plots indicate that the RL and EnKF distributions are comparable, where both cover most of the noisy observations and have the mode of the distribution close to the reference solution. Whereas for $\mathcal{H} = (1, 0, 1)$, the RL distribution is wider covering more of the noisy observations, and has the mode of the distribution closer to the reference solution in comparison to the EnKF solution.

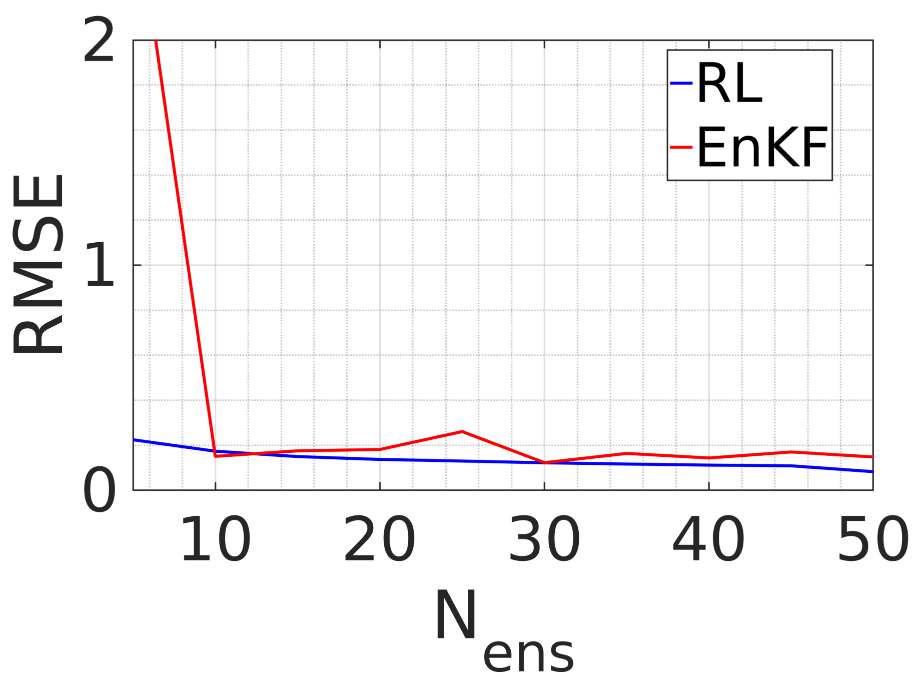

Figure 4: Plot illustrating the RMSE of the ensemble averaged solution as a function of the ensemble size N_{ens}. The plot indicates that the RMSE of the EnKF solution saturates at an ensemble size of 10 meaning that an ensemble size of 50 is considered as a large cardinality ensemble for the Lorenz '63 system. On the other hand, the RMSE of the RL solution appears to keep on decreasing as N_{ens} increases, with a much lower RMSE for small ensembles. This suggests that the RL framework offers huge computational savings with an adequately reliable solution, especially when computational resources are scarce.